Available online at www.sciencedirect.com

SciVerse ScienceDirect

Ceramics International 38 (2012) 4421–4435

CERAMICS INTERNATIONAL

www.elsevier.com/locate/ceramint

Review paper

Review of titania nanotubes: Fabrication and cellular response

A.W. Tan [a], B. Pingguan-Murphy [a,*], R. Ahmad [b], S.A. Akbar [c]

[a] Department of Biomedical Engineering, University of Malaya, 50603 Kuala Lumpur, Malaysia
[b] Department of Mechanical Engineering, University of Malaya, 50603 Kuala Lumpur, Malaysia
[c] Department of Materials Science and Engineering, The Ohio State University, Columbus, OH 43210, USA

Received 9 February 2012; accepted 1 March 2012
Available online 8 March 2012

Abstract

Titania (TiO_2) nanotube is gaining prominence as an implantation material due to its unique properties such as high specific surface area and the ability to exhibit positive cellular response. In this paper, we briefly review the current state of fabrication methods to synthesize nanotubular TiO_2 surface topography, and discuss its effect on cellular response of different cells in terms of cell adhesion, proliferation and differentiation. *In vitro* and *in vivo* studies by using TiO_2 nanotubes are also presented establishing the potential of nanotubes in biomedical applications. Finally, an outlook of future growth of research in TiO_2 nanostructures beyond the nanotubes is provided

Keywords: D. TiO_2; E. Biomedical applications; Cellular response; Nanotube

Contents

1. Introduction

Titanium (Ti) and its alloys have been broadly employed as implantation materials due to their favourable properties such as lower modulus, good tensile strength, excellent biocompatibility and enhanced corrosion resistance compared to 316LSS and Co–Cr alloys [1–6]. However, being bio-inert, they cannot bond with bone directly and do not actively stimulate initialization of bone formation on the surface at an early stage of implantation [7]. They are reported to have a low chemical bonding ability with the bone when employed *in vivo* due to the encapsulation by fibrous tissue that isolates the

* Corresponding author. Tel.: +60 3 7967 4491; fax: +60 3 7967 4579.
E-mail address: bpingguan@um.edu.my (B. Pingguan-Murphy).

0272-8842/$36.00
doi:10.1016/j.ceramint.2012.03.002

implanted material from the surrounding bone and leads to implant dislocation and premature loosening [1,8–10]. Thus, titanium based implants must be able to demonstrate excellent osteointegration at the bone-implant interface, since this is the prerequisite condition for successful clinical implantation. According to Lim et al. and Yu et al., the extent of osteointegration is influenced by the surface properties of the implant [11–14]. Therefore, various surface modifications aimed at improving the osteointegration of the implant's surface have been performed such as sand blasting [15], acid and alkali treatment [16,17], bioactive coating of hydroxyapatite (HA) and calcium phosphate [18], and electrochemical oxidation [19–21].

HA is a virtually ubiquitous bio-ceramic and is extensively used as a bioactive coating on titanium implants due to its chemical and structural similarity to hard tissues, and consequently it can be bonded directly to bone [7]. HA coatings can be deposited by plasma spraying [22], the sol–gel method [18] and ion implantation [23]. Nevertheless, the coating is easily removed from the titanium surface with delamination usually occurring at the interface of bone and implant because there is no interaction between the coating and the substrate [7,24,25]. Bjursten et al. also reported that it is difficult to make HA coatings to remain adherence on Ti due to the difference in mechanical moduli at the HA-Ti interface [24].

Recently, researchers have started to focus on surface modification of the implant in the nano-scale regime because of the natural physiological environment to which bone cells are accustomed to [3,4,26]. Bone is a nanostructured composite matrix which is composed of non-stoichiometric inorganic calcium phosphate mineral and organic protein and collagen [27,28]. Early work done by Webster et al. showed that osteoblast function on nano-phase alumina and titania were significantly improved compared to conventional ceramics [29]. In another study, the group found that osteoblasts showed increased adhesion on nano-phase metals than on conventional metals [30]. These results indicate that nanostructured surfaces can improve osteointegration of the implant. It is believed that high surface area of the nanostructured surface topography provides available sites for protein adsorption and thus enhances the cell-implant interaction [31].

Synthesis of nanostructured titanium dioxide (TiO_2) such as nanotubes, nanowires and nanofibers has raised interest lately due to their high surface-to-volume ratio and the ability to provoke a greater degree of biological plasticity compared to conventional microstructures [32,33]. According to Brammer et al., a physical advantage of a TiO_2 nanostructured surface is that it is composed of and created directly from the underlying native Ti oxide and this can eliminate the tendency of delamination that occurred prevalently in the bioactive coating that were mentioned previously [33].

Nanostructured TiO_2 has been widely used in various applications such as biosensors [34], solar cells [35], photocatalysis [36,37], photoelectrolysis [38] and biomaterials [39,40]. Anatase, rutile and brookite are three common crystal structures of TiO_2. A considerable number of studies have proved that surfaces comprised of nanostructured TiO_2 exhibit positive effect on cell behaviour such as significant accelerated rate of apatite formation, enhanced osteoblast adhesion, proliferation and differentiation [25,33,41–44]. Accordingly, these findings strongly suggest the use of nanostructured TiO_2 as a future implant material.

The aim of this paper is to review a number of established methods for fabrication of biomaterials with nanostructured TiO_2 surface topography. Specific focus is given to TiO_2 nanotubes. The role of surface nano-topography on cellular interaction and biological response of different types of cells is also discussed. Finally, an outlook of future growth of research in TiO_2 nanostructures beyond the nanotube is provided.

2. Fabrication of TiO_2 nanotube

Currently investigated methods of fabricating TiO_2 nanotubes include the assisted-template method [45–47], electrochemical anodic oxidation [26,48–50] and hydrothermal treatment [51–55]. A comparison of these three methods along with their advantages and disadvantages is summarized in Table 1.

Table 1
Comparison of TiO_2 nanotube fabrication methods.

Fabrication method	Advantages	Disadvantages
Template-assisted method	(1) The dimension of nanotubes can be controlled by the dimension and type of templates used	(1) Large nanotubes are obtained
	(2) Nanotubes formed are of uniform sizes	(2) Time consuming due to prefabrication and post-removal of the templates
		(3) Contamination may occur during dissolution of template
Anodization	(1) Dimension of nanotubes can be controlled by varying voltage, electrolyte, pH and anodizing time	(1) Nanotubes produced are in amorphous phase
	(2) Nanotubes produced are aligned with a high aspect ratio	(2) Annealing is required to crystallize the nanotubes produced but lead to collapse of structure at elevated temperature
Hydrothermal treatment	(1) Pure phase nanotubes with good crystallinity can be obtained	(1) Long reaction time is needed
		(2) Concentrated NaOH must be employed that can lead to excessive intercalation causing non-aligned nanotubes

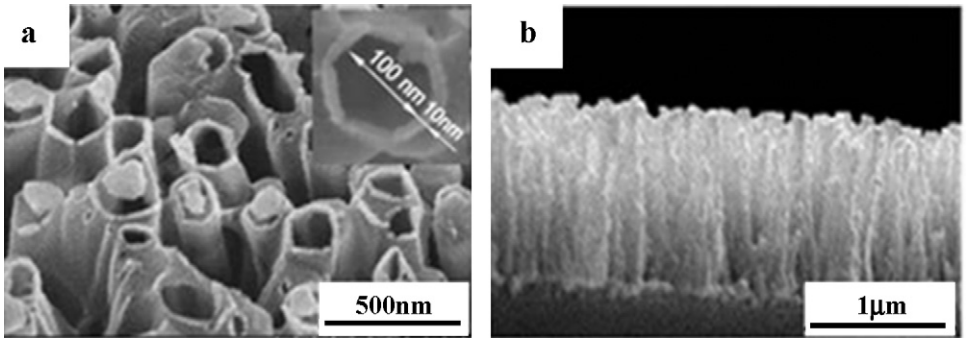

Fig. 1. FESEM image of the ordered array of TiO_2 nanotube arrays (a) after wet-chemical etching and (b) cross-section view [58]. Reprinted with permission from IOP Publishing Ltd.

2.1. Assisted-template method

For the assisted-template method, it can be divided into two types: positive and negative templates. Positive template synthesis is employed when oxide materials are coated on the outer surface of the template, whereas oxide materials are deposited on the surface inside the template's pores when negative template is used [56]. Anodic aluminium oxide (AAO) membrane that consists of an array of monodisperse cylindrical pores with uniform diameter and length is usually used as a template [27,56,57]. The dimension (diameter and length) of the TiO_2 nanotubes can be controlled by the dimension and types of the templates.

2.1.1. Positive template

The synthesis of TiO_2 nanotubes by this method was first reported by Hoyer [45] by employing anodically grown aluminium oxide as the starting material. AAO served as the template to produce a polymer mould. Then, amorphous TiO_2 was electrochemically deposited onto the polymer mould. After dissolution of the polymer mould by using acetone, TiO_2 nanotubes were successfully produced. The nanotubes produced had a length of 8 μm, inner diameter around 70–100 nm and outer diameter between 140 and 180 nm. The author found that the nanotubes consisted of nanocrystalline anatase particles after heat treatment at 450 °C.

Lee et al. reported a one-step templating synthetic strategy to synthesize TiO_2 nanotubes on silicon substrate by utilizing ZnO nanorods as the template. By using this "one-step" method, TiO_2 nanotubes can be obtained without using the chemical medium to dissolve the template, which is different from other template-assisted methods. The ZnO nanorod template was dissolved by the reaction with hydrogen ions (H^+) during the TiO_2 deposition *via* liquid phase deposition (LDP) process. The wall thickness of TiO_2 nanotubes produced was found to range between 50 and 120 nm by varying the deposition time of 3–10 h [47].

Qiu et al. fabricated sol–gel TiO_2 nanotubes on a glass substrate by using ZnO nanorod as positive templates [58]. TiO_2 sol was first deposited on a ZnO nanorod template and then by selectively removing the ZnO template through wet-chemical etching, the TiO_2 nanotubes were obtained. The TiO_2 nanotubes produced were 1.5 μm long and 100–120 nm in inner diameter, with a wall thickness of around 10 nm. Fig. 1 shows the FESEM image of the TiO_2 nanotubes obtained.

By employing positive template, the inner diameters and the length of the resulting nanotubes are determined by the outer diameters and the length of the templates. The thickness of the deposited wall layers is responsible for the outer diameter of the nanotubes. However, the nanotubes obtained by using this approach do not have a uniform length and open ends and thus negative template was introduced [56].

2.1.2. Negative template

Negative templating approach usually produces nanotubes with excellent size uniformity in diameter and length. By combining sol–gel method with AAO as a negative template, Zhang et al. successfully fabricated TiO_2 nanotubes with diameter of about 200 nm and length of about 8 μm [59]. In their experiment, the wall thickness of TiO_2 nanotubes was controlled by the content of acetylacetone (ACAC) in the TiO_2 sol. TiO_2 nanotubes with thin wall of 15–20 nm were obtained when the molar ratio of ACAC in the sol was decreased.

Li et al. synthesized well-aligned anatase TiO_2 nanotubes by sol–gel method using AAO as a negative template [60]. The AAO template was first dipped into the TiO_2 sol for 2 min. After that, the template was removed from the sol under vacuum until the entire volume of the sol was pulled through the AAO template. The AAO template was then dried in air for 30 min at room temperature, calcined in a furnace at 400 °C for 6 h and cool down to room temperature. TiO_2 nanotubes were produced after the AAO was dissolved in NaOH solution. The resultant nanotubes were uniformly distributed and had a wall thickness of about 10 nm and a diameter of around 100 nm, which were exactly the same as the pore size of the AAO template. Similar studies have been conducted by Maiyalagan et al. [61]. From their result, an ordered array of TiO_2 nanotubes with uniform diameter of around 200 nm and length of around 60 μm were formed.

However, both of these assisted-template methods have the disadvantage that it is not easy to obtain smaller nanotubes due to the restriction of the pore size of the mould prepared from porous materials such as alumina [62,63]. Moreover, this method often requires long duration and cumbersome processes for prefabrication and post-removal of the templates. The

removal of the templates is done by using chemical medium and this can lead to contamination since impurities cannot be completely removed during the process [27,47,57,64].

2.2. Anodization

TiO_2 nanotubes with ordered alignment and high aspect ratio had been produced by using anodization [27,57]. The dimension of nanotubes such as the tube diameter and length can be controlled by applying different electrolyte composition, applied voltage, pH and anodizing time based on the investigations by a group of researchers [33,48,49,65].

In the study by Gong et al., well aligned high density TiO_2 nanotubes were obtained by anodizing a pure titanium sheet in an aqueous solution containing 0.5–3.5 wt% hydrofluoric acid [48]. The nanotubes produced had an average diameter ranging from 25 to 65 nm and the trend was found to increase with increasing applied voltage. However, they also concluded that the length of the nanotube was unaffected by anodization time.

Self-organized porous TiO_2 nanotubes (π-TiO_2) were synthesized by Ghicov's group [49] based on the anodization of Ti foil in phosphate/fluoride mixed electrolytes. They reported that nanotubes with a diameter of around 50 nm and a length of up to 500 nm were formed in a H_3PO_4 based electrolyte. Changing the electrolyte to $(NH_4)\,H_2PO_4$ led to the formation of nanotubes with a diameter around 100 nm and a length of up to 4 μm. Furthermore, they also showed that the thickness of the nanotube layers was affected by the pH dependence of the oxide dissolution rate and anodization time. The dissolution rate at low pH (H_3PO_4) was much higher than high pH ($(NH_4)\,H_2PO_4$).

Bauer et al. investigated the effect of fluoride concentrations and applied potentials in H_3PO_4 electrolyte on the formation of self-assembled TiO_2 nanotube layers [65]. They deduced that the optimized condition for self-organized TiO_2 nanotube formation was established for 0.3 wt% HF and tube diameter and length depended linearly on the applied voltage from 1 V to 25 V. The anodic layer did not show a self-organized morphology at potentials higher than 25 V.

Nevertheless, the main disadvantage of this method is that the as-synthesized nanotubes are amorphous and a post-annealing is required to crystallize them into anatase, rutile or bookite structure [27]. Also, some studies showed that the annealing had an adverse effect on the stability of nanotubular structure [1,10]. At elevated temperature, high surface area makes the nanotubes prone to solid-state sintering, which leads to grain growth, densification and eventually complete collapse of the nanotubular structure [50].

2.3. Hydrothermal treatment

Hydrothermal treatment has received wider attention because this method yields pure phase TiO_2 nanotubes with good crystallinity [27]. This method has been reviewed in detail by Ou et al. and Wong et al. [57,63]. The formation of TiO_2 nanotubes by using hydrothermal treatment is affected by the starting materials [66,67], sonication pre-treatment [68], hydrothermal temperature [69] and post-treatment [54,70–72].

Tsai and Teng prepared TiO_2 nanotubes by hydrothermal treatment of commercial TiO_2 nanoparticles in NaOH followed by HCl washing [51]. A hydrothermal temperature ranging from 110 to 150 °C showed effects on the extent of particle-to-sheet-to-tube conversion and the anatase-to-rutile transformation. They found that surface area of the nanotubes increased with the treatment temperature and reached a maximum of about 400 m^2/g at 130 °C. Based on their study, they found out that NaOH treatment was used to break the Ti–O–Ti bond in the nanoparticles to form Ti–O–Na and Ti–OH bonds [62,73]. This rupture led to the formation of TiO_2 sheets due to the electrostatic repulsion of the charge on sodium. The sheets then scrolled to become TiO_2 nanotubes after HCl washing due to the removal of electrostatic charges of the TiO_2 sheet as confirmed by TEM observation.

In another study, Poudel et al. synthesized TiO_2 nanotubes with an outside diameter of ∼9 nm, wall thickness of ∼2.5 nm and length of ∼600 nm by using anatase nanopowder and micropowder as starting material using a hydrothermal method [54]. The spacing between layers of the wall was found to be in the range of 0.70–0.75 nm. They concluded that the crystallinity of nanotubes was strongly affected by the volume of solution in the autoclave (filling fraction) while the impurities depended on the acid treatment. Acid washing was required in order to produce high yield and pure nanotubes. According to their observation, the volume filling fraction had to be more than 0.84 and treated with 0.5–1.5 M HCl to obtain nanotubes with high purity and crystallinity when micropowder was employed as the starting material. The volume filling fraction had to be increased up to 0.90 when changing the starting material to nanopowder. In addition, annealing was done for the purpose of nanotube stability study. In this context, they observed that the anatase phase of the as prepared nanotubes was stable up to 700 °C and the tubular morphology started to change to nanowires with diameter more than 20 nm when the temperature was above 550 °C as shown in Fig. 2. However, no explanation is reported for this transformation.

Tsai and Teng investigated the role of post treatment acidity on the structural features of the nanotubes synthesized by using hydrothermal method [52]. Some researchers [51,74,75] had reported that acid washing was the key to nanotube formation, while others [76–78] concluded that acid washing was not important. Tsai and Teng postulated that the difference in the severity of the NaOH treatment such as the difference in temperature and the duration employed are the main reasons for the contradiction observed between these previous studies. In this work, they demonstrated that titanate ($Na_2Ti_2O_5{\cdot}H_2O$) nanotubes were formed after HCl acid washing and the nanotubes became defective and transformed into nanocrystalline anatase with turbostratic stacking when the acidity of the washing was increased. However, they successfully transformed the nanocrystalline anatase into TiO_2 nanotubes by backwashing with NaOH. This finding showed that transformation between titanate–titania nanotubes could be achieved through a soft-chemical reaction route.

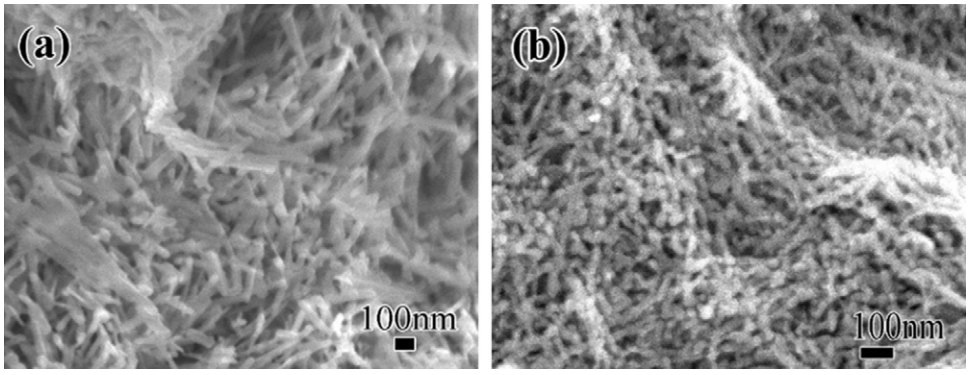

Fig. 2. SEM image (a) nanotubes synthesized under optimal autoclave condition and treated with 0.1 M HCl and annealed at 650 °C; (b) similar samples but treated with 1 M HCl showing the morphology transformation into nanowires [54].
Reprinted with permission from IOP Publishing Ltd.

However, this nanotube fabrication method is reported to have some disadvantages such as the requirement for long reaction times and the need for NaOH, which can lead to excessive intercalation that can produce nanotubes that are in powder form of random alignment [27,57].

3. Cellular response to TiO_2 nanotubes

Titanium and its alloys have been widely used in numerous clinical implantation devices, including bone and joint replacement, dental implants, prostheses, cardiovascular implant and maxillofacial and craniofacial treatments as shown in Fig. 3 [79,80]. For these applications, the cell-implant interaction is important for successful clinical implantation. The influence of TiO_2 nanotubes on cellular response has been investigated using a variety of cell types including osteoblasts [1,2,10,11,25,33,41,81–83], fibroblasts [84], chondrocytes [85,86], endothelial cells [87], muscle cells [87], epidermal keratinocytes [84] and mesenchymal stem cell (MSC) [32,88–91]. Selected *in vitro* studies are summarized in Table 2. At the end of this section, a few *in vivo* studies using TiO_2 nanotubes are also discussed.

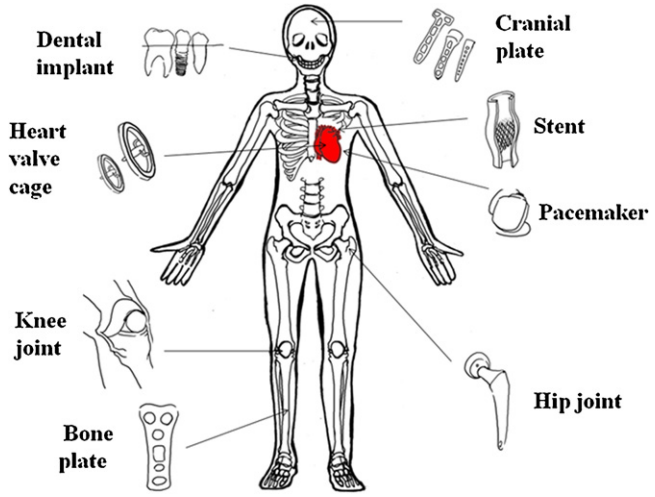

Fig. 3. Biomedical application of titanium and its alloys.

3.1. Osteoblasts

Oh et al. carried out their studies on the growth of MC3T3-E1 mouse preosteoblasts by using anodized TiO_2 nanotubes [25]. The dimension of the produced nanotubes averaged 100 nm outer diameter and 70 nm inner diameter, with 15 nm wall thickness and 250 nm height. The TiO_2 nanotubes were found to consist of the anatase crystalline phase after being heat treated to 500 °C for 2 h in air. The adhesion/propagation of the osteoblasts was significantly improved by the presence of TiO_2 nanotube topography with the filopodia of the propagating osteoblasts growing into the pores of the nanotubes and forming an interlocked cell structure. The number of adherent cells on the TiO_2 nanotubes increased by ~300–400% compared to the unanodized Ti-control surface according to back scattered SEM micrographs. TiO_2 nanotubes were discrete in structure, with a gap of ~15 nm between adjacent nanotubes, leading to speculation that these gaps serve as pathways for continuous supply of body fluid and nutrient, which are essential biological elements for cell growth.

In further studies by the same group, the possibility of enhancing the bioactivity of TiO_2 nanotubes by exposing them to 5 mol NaOH solution at 60 °C for 60 min was investigated [81]. The nanotubes were heat treated at 500 °C for 2 h to obtain anatase TiO_2 nanotubes. The findings indicate that sodium titanate nanofibers grew on the edge of the anodized TiO_2 nanotubes after the exposure to the NaOH solution. In order to evaluate bone growth on bioactive surfaces in terms of hydroxyapatite formation, a stimulated body fluid (SBF) test was conducted. The results indicated that the formation of HA on the TiO_2 nanotubes surface containing sodium titanate was significantly accelerated by a factor of 7 as compared to the same TiO_2 nanotubes surface without sodium titanate. This finding suggests that formation of sodium titanate nanostructure has an effect in accelerating *in vitro* hydroxyapatite formation.

Das et al. studied the effect of anodized TiO_2 nanotubes on human osteoblasts (HOB) by using an osteo-precursor cell line (OPC1) that was established from human foetal bone tissue [2]. The TiO_2 nanotubes were grown by anodization at 20 V for duration of 2 and 4 h. The produced nanotubes had the inner

Table 2
Cell behaviour of TiO_2 nanotubes on different cells.

Cell type	Cellular response	Reference
Osteoblast	Accelerated cell adhesion and growth with faster propagation of filopodia on the TiO_2 nanotubes structure compared to Ti sample.	[25]
	NaOH is added after the anodization. Growth of sodium titanate nanofiber was observed on the TiO_2 nanotube edge and it accelerated the formation of hydroxyapatite after subjected to SBF.	[81]
	Increased cell adhesion, proliferation and ALP activity. Apatite layer was formed on TiO_2 nanotube surface but it was nonuniform in SBF.	[2]
	Cell adhesion, ALP activity and mineralization increased with nanotube diameter from 20 to 70 nm and reached a maximum on nanotubes with 70 nm diameter. However, such observations become limited beyond 70 nm and reached lowest on 120 nm. Surprisingly, the cell proliferation rate increased with increasing nanotube diameter from 20 to 120 nm.	[11]
	Cell attachment, viability, proliferation and mineraization showed the trend of anatase-rutile > pure anatase > amorphous nanotubes.	[1]
	Highest cell activity (cell attachment and proliferation) was observed on the TiO_2 nanotubes annealed at 600 °C which is a mixture of anatase-and-rutile phase.	[96]
	TiO_2 nanotubes of 30 nm in diameter showed the highest degree of cell adhesion and proliferation, while larger diameter nanotubes (70–100 nm) elicited a lower cell population with extremely elongated cellular morphology and higher ALP levels. TiO_2 nanotube with 100 nm had the highest ALP level.	[33]
Chondrocyte	Increased cell adhesion on anodized TiO_2 nanotube structure compared to un-anodized Ti sample.	[85]
	Dense extracellular matrix (ECM) fibrils were found on TiO_2 nanotube substrate. TiO_2 nanotube with diameter of 70 nm showed the highest glycosaminoglycan (GAG) secretion, aggrecan and collagen type II transcription level.	[86]
Fibroblast and epidermal keratinocyte	Nanotube topography is favourable for the growth and maintenance of dermal fibroblast but not for epidermal keratinocyte. Increased dermal fibroblast and decreased epidermal keratinocyte adhesion, proliferation and differentiation were observed.	[84]
Endothelial and muscle cells	Pronounced protrusion of filopodia and increased ECM deposition on TiO_2 nanotube were observed. Actin filaments were found to form unidirectional cytoskeletons and more organized lamellipodia on the nanotube surface. The NO_x and endothelin-1 functional assays confirmed that the nanotube structure could up-regulate an antithrombotic cellular state for maintaining vascular tone.	[40]
	Endothelial cells were observed to have elongated morphologies on nanotubular substrate, whereas muscle cells had more rounded cell on nanotubes than on the control flat Ti surface. Endothelial growth was favourably enhanced on nanotubular morphology while decreasing muscle cell proliferation, migration and function.	[87]
Mesenchymal stem cell (MSC)	TiO_2 nanotube with diameter of 15 nm gives the optimum results for integrin clustering and focal formation, including cell proliferation, migration and differentiation into osteogenic lineages.	[88]
	Differentiation of both MSC and HSC to osteoblasts and osteoclasts were significantly stimulated by nanotubes below 30 nm and severely inhibited by larger diameter.	[82]
	Maximum cell activity (adhesion and proliferation) was achieved on TiO_2 nanotube diameters of 15 nm regardless of the type of material surface. Cell behaviour was not affected by the tube length since the number of adherent cells on the different nanotube surfaces was found to be in a comparable range for different tube lengths.	[91]
	Higher rate of cell adhesion, proliferation, ALP activity and bone matrix deposition was found on TiO_2 nanotubular surface compared to a flat Ti surface.	[89]
	Increased cell adhesion was observed on smaller diameter nanotubes (~30 nm) but osteoblasts differentiation was prevalent on larger diameter nanotubes (70–100 nm).	[32]
	Osteoblasts were found to have a higher ALP activity on the TiO_2 nanotube surface, while MSCs had the highest osteogenic differentiation on the carbon coated TiO_2 nanotubes.	[41]

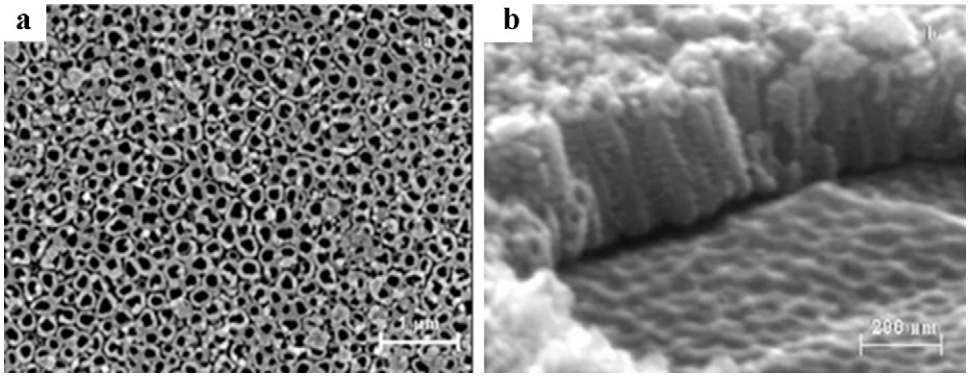

Fig. 4. FESEM image of (a) Top-view of nanoporous TiO_2 film anodized at 20 V for 4 h. (b) Cross-sectional of the same film showing the length of the TiO_2 nanotubes on Ti [2].
Reprinted with permission from John Wiley and Sons Inc.

diameter of 51–54 nm, a length of 288–600 nm and a wall thickness of 39–51 nm. Fig. 4 shows the FESEM image of anodized TiO_2 nanotubes at 20 V for 4 h. It was found that the length of the nanotubes increased with increasing anodization time initially, but the nanotubular structure collapsed beyond 4 h of anodization. For the evaluation of bone cell-material interaction, the authors chose nanotubes that were grown in 4 h as it showed uniform nanoporous structure and better surface properties. The nanotubes were then crystallized into rutile phase at 580 °C. The nanotubes showed better cell spreading and adhesion by forming filamentous network structures that acted as excellent anchorage sites for the filopodia extension as shown in Fig. 5. The nanoscale morphology also exhibited early differentiation by showing increased alkaline phosphatase (ALP) activity and statistically significant bone cell proliferation as indicated by MTT assay compared to a polished Ti-control surface. All these results indicate that a nanotubular structure of Ti is more osteoconductive than conventional polished Ti surface.

Yu et al. evaluated MC3T3-E1 preosteoblast behaviour in terms of adhesion, proliferation and differentiation on different diameter anatase-TiO_2 nanotube layers produced by anodizing the Ti surface at a series of voltage ranging from 5 to 25 V [11]. The diameter of nanotube layers were approximately 20, 50, 70, 100 and 120 nm with a wall thickness of 100, 250, 300, 400 and 450 nm, respectively. The as-fabricated nanotubes were then heat treated at 450 °C for 3 h to obtain anatase TiO_2 nanotubes. The MC3T3-E1 preosteoblasts adhered well on the tubes of diameter 20–70 nm. Cell attachment and spreading was minimal on the tubes of diameter larger than 70 nm. The same trend was observed for cell differentiation. The ALP activity of MC3T3-E1 preosteoblasts was suppressed when the tube diameter was larger than 70 nm. Based on the results from the cell adhesion and ALP activity studies, the authors hypothesized that tube diameter of 20–70 nm provide proper dimensions for integrin clustering. Cells are in contact with the ECM *via* integrins and thus clustering of integrins leads to the focal contact formation, which can induce higher rate of cell adhesion and differentiation. However, to their surprise, the proliferation of MC3T3-E1 preosteoblasts showed a different tendency with cell adhesion and ALP activity. The cell proliferation rates increased with increasing diameter of nanotubes. These findings demonstrate that cells may respond individually to different sizes of TiO_2 nanotube.

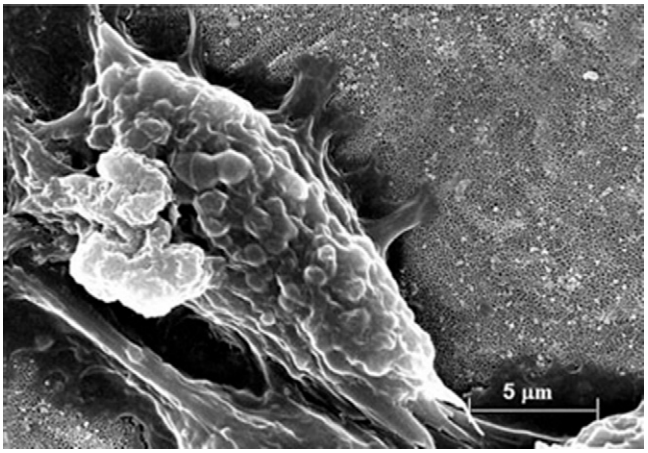

Fig. 5. OPC1 human osteoblast cell attachment after 11 days on nanoporous TiO_2 surface at high magnification. Filopodia from cells use the nanoporous areas as anchorage sites for attachment [2].
Reprinted with permission from John Wiley and Sons Inc.

The evaluation of osteoblast behaviour on different crystal structure of TiO_2 nanotubes has been conducted by Yu et al. [1]. The anodized TiO_2 nanotubes were annealed at 450 °C, 550 °C and 650 °C for 3 h in air in order to acquire different crystalline phases of nanotube. Initially, the unannealed nanotubes had an amorphous structure. The amorphous structure was converted into an anatase structure after annealing at 450 °C and to a mixture of anatase and rutile after annealing at 550 °C. However, the tubular morphology collapsed when annealed at 650 °C. The results showed that MC3T3-E1 preosteoblasts spread better and extended more filopodias on the nanotubes surface according to the trend following: anatase-rutile > pure anatase > amorphous nanotubes. The same results were observed for cell proliferation and mineralization as measured by MTT assay and Alizarin Red-S (ARS) staining. From this study, the authors concluded that the crystal structure plays a role in cell-material interaction. Similar observations were shown in the study of Bai's group [10]. Bai et al. annealed the anodized TiO_2 nanotubes at 450, 600 and 750 °C for 2 h at a

heating rate of 10 °C/min in air. They also observed that crystallization of the nanotubes to the anatase phase occurred at 450 °C, while a mixture of anatase-rutile formation was observed at 600 °C. The nanotubular structure collapsed completely at 750 °C. The SBF study showed that TiO_2 nanotubes with a mixture of anatase-rutile were more efficient in promoting the apatite formation than plain anatase or amorphous structure. The highest MC3T3-E1 preosteoblast cell activity was obtained on the TiO_2 nanotubes annealed at 600 °C.

Another study of osteoblast cellular behaviour in response to different nanotube sizes has been carried out by Brammer et al. [33]. Highly ordered, vertically aligned nanotubes with pore sizes of 30, 50, 70 and 100 nm were fabricated by controlling the anodizing potential at 5, 10, 15 and 20 V for 30 min. The anatase phase of TiO_2 nanotubes was obtained after heat treatment at 500 °C for 2 h. Their results showed that 30 nm TiO_2 nanotubes had the highest degree of cell adhesion and proliferation, while larger diameter nanotubes (70–100 nm) exhibited a lower cell population with extremely elongated cellular morphology and higher ALP levels. They found that the phenomenon of adhesion *versus* elongation was determined by initial adsorption of proteins (fibronectin and albumin) from the serum in the culture medium [32,33]. From their SEM micrographs, proteins had adhered sparsely to the top wall surface on the 100 nm TiO_2 nanotubes due to the presence of large nanopores and the osteoblasts had to expand their filopodia to find this protein-deposited surface, thus forming an elongated cellular morphology. They further postulated that there may be a relation between initial protein adsorption, the cell elongation and the ALP activity because similar trends were shown from the results of elongation and ALP activity tests. The 100 nm TiO_2 nanotubes had increased elongation and the highest ALP functionality leading to the conclusion that 100 nm diameter nanotubes had the greatest potential for use as bone implants.

3.2. Chondrocyte

The investigation of adhesion of chondrocyte to TiO_2 nanotubes was first reported by Burns et al. [85]. The amorphous TiO_2 nanotubes were synthesized by anodizing the Ti substrate at 20 V for 20 min. SEM micrographs showed that the nanotubes produced were between 100 and 200 nm deep and had an inner diameter around 70–80 nm. Human articular chondrocytes were employed as cell cultures in this study. Based on their results, 40% more chondrocytes were counted on anodized TiO_2 nanotubes compared with unanodized Ti. Nanotubes morphology provided a higher surface area of reactive sites for initial protein interaction, potentially mediating chondrocyte adhesion. Such morphology also affects the surface wettability and surface potential, both of which are known to influence initial protein adsorption leading to increased chondrocyte adhesion. Further studies need to be conducted to optimize for improved chondrocyte functionality.

To explore the effect of the pore size of TiO_2 nanotubes on the bovine cartilage chondocyte (BCC) cells, Brammer et al. [86] fabricated four different pore diameters (30, 50, 70 and 100 nm) by anodization as described in their previous studies [33]. The samples were crystallized into the anatase phase by heat treating at 500 °C. Their SEM observations showed that BCCs produced dense extracellular matrix (ECM) fibrils on the nanotube substrate, which were lacking on flat control Ti because the nanotube substrate contained fine scale cues that aid in signalling ECM fibril production and organization. Round, spherical cells were observed on the TiO_2 nanotube surface, whereas fibroblastic shaped cells were observed on the flat control Ti. The reason proposed by the authors was that cells adhered strongly on the amorphous flat surface and so spreading occurred, but less strongly on the crystallized surface allowing them to retain round shape due to prevention of chondrocyte spreading. Besides, the biochemical ECM examination revealed that glycosaminoglycan (GAG) secretion in the culture medium was also increased on the nanotube substrate, reaching the highest production on the 70 nm diameter nanotubes with ~100% increase in GAG secretion than on flat Ti. PCR analysis was performed for two chondrogenic markers namely aggrecan and collagen type II to ensure no loss of phenotype on the experimental substrate. From the PCR anlaysis, nanotube substrate had significantly shown higher level of aggrecan and collagen type II transcription level. Again, 70 nm diameter nanotubes exhibited the highest level of both chondrogenic transcription levels. Therefore, the authors concluded TiO_2 nanotubes in the range of 70 nm diameter could be the most promising biomaterial in cartilage–bone interface osteochondral treatments.

3.3. Fibroblast and epidermal keratinocyte

Titanium and its alloys are the most commonly used biomaterials for transcutaneous implants [92,93]. As a transcutaneous implantable device, they are always in constant contact with the thick underlying dermal layer of the skin, consisting of fibroblasts, and the thin external layer, consisting of keratinocytes. Therefore, the response of human dermal fibroblasts (HDF) and human epidermal kerationocytes (HEK) on the TiO_2 nanotubes has been studied by Smith et al. [84]. The nanotubes were synthesized by anodization and annealed at 530 °C for 3 h to obtain crystallized nanotubes. The SEM results indicated that the nanotubes had a length of approximately 1–1.5 μm and a diameter of 70–90 nm. Cellular responses in terms of adhesion, proliferation, differentiation and cytoskeleton organization for up to 4 days culture were studied. The results showed that cell adhesion on TiO_2 nanotube substrate was increased by 14% in HDF and decreased by 43% in HEK when compared to the control Ti substrate. Similarly, as indicated by MTT assay, cell proliferation rate was increased in HDF but decreased in HEK on TiO_2 nanotubes substrate compared with the control substrate. The authors believed that cellular response with TiO_2 nanotubes resulted in cytoskeleton reorganization and thus a comparative investigation between the control substrate and 4 days culture TiO_2 nanotube substrate was undertaken by staining them with anti-vinculin (vinculin stain) and rhodamine-conjugated phalloidin (F-actin stain). The results revealed

increased expression of vinculin and F-actin by HDF cells on TiO_2 nanotube arrays compared to the control substrate, identifying enhanced cytoskeleton reorganization and membrane protein expressions on TiO_2 nanotube arrays. However, the opposite observation was found in HEK cells. HEK cells showed minimal expression of vinculin and F-actin and lack of cytoskeleton reorganization. In this study, the cell differentiation was characterized by indirect immunofluorescence staining of specific marker proteins that are known to be expressed in activated HDF and HEK cells. HDF cells expressed collagen Iα1 and fibrilin 1 while HEK cells expressed cytokeratin 19 and laminin β3. The results again indicated an increase in collagen Iα1 and fibrilin 1 expression in HDF cells and decrease in cytokeratin 19 and laminin β3 on TiO_2 nanotube substrates compared to the control substrate. Overall, this study found that the nanotube topography provides a favourable template for the growth and maintenance of HDF cells but not for HEK cells. The authors suspected that the cuboidal, non-elongated structure of HEK cells were unable to interact with the nanotube topography optimally and thus resulted in decrease of HEK cell functionality on TiO_2 nanotubes substrate.

3.4. Endothelial and muscle cell

Brammer et al. carried out a comparative study of flat Ti and a TiO_2 nanotube substrate using primary bovine aortic endothelial cells (BAECs) [40]. The TiO_2 nanotubes were prepared by anodization. BAECs showed significant improved interaction with the TiO_2 nanotube surface by showing enhanced cellular migration and functioning as compared to a flat Ti surface. Pronounced protrusion of filopodia and increased ECM deposition were found on the TiO_2 nanotubes surface due to the ability of nanotube surface to provide nanocues that can facilitate endothelial cell sensing, spreading, attachment and migration. From the results for actin, actin filaments were found to form unidirectional cytoskeletons and more organized lamellipodia on the nanotube surface. This implies that nanotube surface had the advantage over the flat surface in allowing for more dynamic and coordinated changes in cytoskeleton organization, locomotion and cell-to-cell communication. As a homeostatic environment is important for cells to function properly, the release of nitrogen oxide (NO_x) and endothelin-1 was investigated in this study. NO_x is an important vasodilator that inhibits platelet aggregation whereas endothelin-1 serves as vasoconstrictor that promotes platelet aggregation. The NO_x and endothelin-1 functional assays confirmed that the nanotube structure could up-regulate an antithrombotic cellular state for maintaining vascular tone. These findings suggest that a TiO_2 nanotube structure has the potential to be used as a vascular stent material.

Currently, clinically used surface modifications of vascular prostheses such as stents or vascular grafts are aimed at deceasing vascular smooth muscle cells proliferation at the expense of endothelial cells proliferation, migration and function. Therefore, Peng et al. investigated the effect of TiO_2 nanotube surface on endothelial function and smooth muscle proliferation by employing bovine aortic endothelial and mouse aortic vascular smooth muscle (MOVAS) cell culture [87]. BAECs were observed to have elongated morphologies on nanotubular substrate, whereas MOVASs had more rounded cell on nanotubes than on the control flat Ti surface. This observation indicated that muscle cells, that are MOVAS in this study, were less likely to thrive and proliferate on nanotube substrate. The proliferation assay was examined by using 5-ethynyl-2′-deoxyuridine (EdU). The results showed that BAECs increased proliferation rate on nanotubes initially, but returned to the same level to that of the cells on flat Ti surface. In contrast, MOVASs showed a significantly decreased rate. These results suggested that endothelial growth was favourably enhanced on nanotubular morphology while decreasing muscle cell proliferation. The differentiation of muscle cells was evaluated by using a special marker, smooth muscle α-actin (SMαA) and increased level of SMαA expression was observed on TiO_2 nanotubes by approximately three fold as compared to control Ti substrate. This demonstrated that nanotubes aid in maintaining the differentiated state of muscle cells and non-proliferative phenotype. According to the authors, the primary function of endothelial cells is to secret products that prevent clotting and inhibit muscle cell proliferation such as nitric oxide (NO) and prostaglandin I_2 (PGI_2). Therefore, the effect of nanotubes on the function of endothelial cells was investigated by using PGI_2 secretion. Clearly, the results showed that nanotubes increased the secretion of PGI_2 when compared to flat Ti, a very promising finding, as PGI_2 is known to have the ability to reduce clotting. In conclusion, this study has shown that TiO_2 nanotubes have potential for vascular implantation applications.

3.5. Mesenchymal stem cell

Stem cells are unspecialized cells characterized by self-renewal and multipotential differentiation [94]. They can be induced to become cells of a specific lineage under certain microenvironments. MSCs are multipotent stem cells that can differentiate into multiple mesenchymal lineages such as osteoblasts, chondrocytes, endothelial cells, fibroblasts and myocytes [13,32,89]. Therefore, several studies have investigated the influence of TiO_2 nanotube in directing MSC cell fate. Park et al. reported the cellular response to TiO_2 nanotube with six different diameters between 15, 20, 30, 50, 70 and 100 nm by using rat MSCs as cell culture [88]. The nanotubes were prepared by anodizing Ti sheet in a phosphate-fluoride electrolyte at different voltages ranging from 1 to 20 V. They found that cell adhesion and spreading was the highest on 15 nm tubes and declined significantly with increasing pore size. Lamellopodia and filopodia were formed on smaller size diameter (15–30 nm) compared to larger size diameter (50–100 nm). The focal adhesion is vital in regulating intracellular signalling pathways and integrin function. Therefore, the formation of focal contact has been analyzed by using paxillin as a marker protein. A higher extent of focal contact formation was observed on nanotubes smaller than 30 nm. Besides, the cell proliferation rates were found to reach their highest on

15 nm diameter surfaces and decreased with increasing tube diameter. Cell differentiation of MSCs into osteogenic lineages was determined by using Alizarin red. The results again showed that the osteoblast differentiation rate was the highest on 15 nm tubes and lowest on 100 nm TiO_2 nanotubes. This study demonstrated that TiO_2 nanotube with 15 nm diameter provided the optimum length scale for integrin clustering and focal adhesion and led to higher rate of cell proliferation and differentiation.

Park et al. continued to explore the effect of TiO_2 nanotube diameter on stem cell behaviour by comparing the osteoclasts and osteoblasts [82]. Osteoclasts are bone-resorbing cells that are derived from hematopoietic stem cells (HSCs), while osteoblasts are bone-forming cells that are derived from MSCs. In this study, TiO_2 nanotube surface with six different diameters between 15 and 100 nm were used, as described previously [88]. HSC differentiation to osteoclasts was significantly stimulated by nanotubes below 30 nm and severely inhibited by larger diameter. Similar observations were found from differentiation of MSCs to osteoblasts. Since HSCs and MSCs both demonstrated the same size dependence in their response to TiO_2 nanotubes, the authors suggest that a nanotube platform with a diameter of approximately 15 nm would be preferentially recognized by other cells due to a comparable size of integrins with an actual size of about 10 nm diameter [95]. Further study is needed to confirm this finding.

In another study, Bauer et al. investigated the behaviour of MSCs in terms of cell adhesion and proliferation on nanotopographies of different dimensions and different materials [91]. Three types of materials were fabricated, ZrO_2 nanotubes, TiO_2 nanotubes and TiO_2 nanotubes sputter coated with a dense AuPd layer. Nanotube diameters ranging from 15 up to 100 nm with differing lengths were fabricated by controlling the applied potential and electrolytes used during anodization. The results demonstrated that all three surfaces showed an identical nanosize dependence of the cell response, with a maximum cell activity found for tube diameters of 15 nm. This indicated that size effects clearly override the surface chemistry effects. However, the directed differentiation of MSCs was not addressed. The cellular response of MSCs on different nanotubes with different lengths also was investigated in this study. The number of adherent cells on the different nanotube surfaces was found to be in a comparable range for different tube lengths. Thus, the authors concluded that cell behaviour is not affected by the tube length.

Popat et al. demonstrated the ability of TiO_2 nanotubes to promote differentiation of MSCs into osteoblasts [89]. Crystallized TiO_2 nanotubes with pore size of 80 nm and length of 400 nm were produced using anodization at 20 V for 20 min followed by annealing at 500 °C in dry oxygen ambient. Cellular response, in terms of cell adhesion, proliferation and differentiation, was investigated in this study. The results showed that a higher rate of adhesion, proliferation and ALP activity resulted from the nanotubular surface, compared to a flat Ti surface. This was demonstrated by a 40% increase in the number of cells and a 50% increase in ALP levels present on the nanotubular TiO_2 surface compared to flat Ti surface. Therefore, the authors suggested that TiO_2 nanotube surface provides a preferential interface for the differentiation of MSCs into osteoblasts.

Oh et al. elucidated that a guided osteogenic differentiation of human MSCs can be controlled by selective sizing of the TiO_2 nanotube dimensions [32]. Nanotubes of 30, 50, 70 and 100 nm sizes were prepared by anodization and heat treated at 500 °C for 2 h to obtain crystallinezed TiO_2 nanotubes. They observed that, on smaller diameter nanotubes (~30 nm), increased cell adhesion and growth of minimal differentiation seem to be prevalent. This observation may attribute to the higher population of protein aggregates on the top surface of smaller nanotubes since protein aggregates initially attach only to the available surfaces that are the top portion of the nanotube walls. However, on larger diameter nanotubes, hMSCs elicited a lower initial cell number but a higher growth of osteoblasts differentiation. This observation is likely due to the fact that hMSCs were forced to elongate and stretch to search for protein aggregates on larger nanotube structures and as a result, were induced to differentiate into osteoblasts. They consider these findings a milestone for future study of stem cell research and implant development.

Brammer et al. compared the cell behaviour of MSCs and osteoblasts on two different surface chemistries, TiO_2 nanotubes and carbon-coated TiO_2 nanotubes [41]. The anodized nanotubes had an outer diameter of 100 nm, wall thickness of 10 nm, spacing of 10 nm and length of 300 nm. The TiO_2 nanotubes were in the anatase phase whereas carbon coated TiO_2 nantoubes were amorphous. For the *in vitro* evaluation using osteoblasts, they found that adhesion and proliferation of osteoblasts were affected by the nanotopographic structure, while surface chemistry of the material played a role in the functionality. TiO_2 nanotubes had a slight advantage over carbon coated nanotubes in terms of ALP activity. For the *in vitro* evaluation using human MSCs, ALP activity and osteogenic differentiation were employed to examine the directed differentiation of MSCs into osteoblasts. The results showed that carbon coated TiO_2 naotubes induced an obvious increase in relative osteogenic differentiation over the TiO_2 nanotubes. Overall, osteoblasts were found to have a higher ALP activity on the TiO_2 nanotube surface, while MSCs had the highest osteogenic differentiation on the carbon coated TiO_2 nanotubes. The authors hypothesized that MSCs preferred a carbon surface when in undifferentiated mode, but changed to TiO_2 nanotubes once they differentiated into osteoblasts. Therefore, these findings showed that the chemistry of the nanotube surface had a direct effect on the functionality of cells and different cell types had different chemical preference for optimal function.

3.6. *In vivo* studies

Based on the previous studies, TiO_2 nanotubes were reported to increase *in vitro* cell-implant interaction, yet little is known how this nanotubular implant surface can affect the cell-implant interaction *in vivo*. Popat et al. conducted *in vivo* biocompatibility test by implanting discs of Ti and TiO_2 nanotube subcutaneously in male Lewis rat [89]. Histological analysis

was evaluated after 4 weeks of implantation. The results showed that no fibrous tissues were presented in the tissues surrounding TiO_2 nanotubes implant and were comparable to healthy tissues. This preliminary result suggested that nanotubular morphology did not cause any adverse immune response under *in vivo* condition.

In another *in vivo* study, Bjursten et al. compared the TiO_2 nanotube to TiO_2 gritblasted surface by implanting them in rabbit tibias for 4 weeks [24]. The nanotubes produced were found to have ~100 nm outer diameter, ~80 nm inner diameter, ~10 nm wall thicknesses, height of ~250 nm and consisted of anatase structure after annealed at 550 °C. The gritblasted Ti surface was covered with an amorphous TiO_2 layer of ~5 nm thick. Overall, the TiO_2 nanotube implant showed better *in vivo* performance than the gritbalsted TiO_2 surface implant. The tensile test results indicated that a greater fracture force was needed in order to remove nanotube implant from rabbit tibia compared to gritblasted TiO_2 surface. The bone-implant contact area was higher for TiO_2 nanotube surfaces compared to gritblasted surfaces (78.3 33.3% and 21.7 24.7%, respectively). SEM EDX mapping of implant-bone interface was performed after the tensile test. The results revealed that a high concentration of calcium and phosphorus were detected on the TiO_2 nanotube surface, but not on the gritblasted Ti implant surface. This showed that the TiO_2 nanotube had strong interface bonding with bone that the fracture actually occurred within the growing bone, rather than at the implant-bone interface. Based on the histological analysis, the results demonstrated greater bone-implant contact, bone formation and calcium level on the TiO_2 nanotube surfaces as compared to gritbalsted surfaces. Thus, the authors concluded that TiO_2 nanotubes could improve *in vivo* bone bonding tensile strength significantly compared to gritblasted Ti surfaces.

A similar *in vivo* study was carried out by Wilmowsky et al. by using adult domestic pig as animal model [97]. The pig model was chosen due to its comparable morphological and anatomical characteristics with humans. In this study, the effect of surface morphology on peri-implant bone formation *in vivo* was investigated by comparing TiO_2 nanotube surfaces with an untreated standard Ti surface. The TiO_2 nanotube surfaces were prepared by anodization and had a diameter of 30 nm. Expression of collagen type-1 and osteocalcin were performed to evaluate the time sequence in the bone regeneration process. The expression of collagen type-1 was known to be an early indicator of *de novo* bone formation, while osteocalcin was described as a late marker of bone development. Their results showed that anodic TiO_2 nanotubes were able to stimulate bone formation around the implant surface by showing a higher expression rate of collagen type-1 than the standard Ti surface at an early stage of bone formation. Thereby, it is believed that TiO_2 nanotube surfaces could have an accelerating effect on the differentiation of the surrounding osteoblasts and might provoke fast new bone formation around Ti implants. Nevertheless, no obvious difference could be observed at any point of time for the expression of osteocalcin for both the implant surfaces. This might indicate that nanotubular surfaces did not affect the mineralization process during bone development and remodelling. From the bone-implant contact analysis, it can be observed that the amount of bone formation of both implant surfaces was similar with no statistical differences at any point of time throughout the study. Thus, the authors concluded that TiO_2 nanotube in 30 nm diameter could enhance the osteoblast function, but not the cell proliferation rate. Further *in vivo* study is needed to investigate the optimal size range of TiO_2 nanotube diameter that is capable of modulating both cell proliferation and function.

Currently, the effects of TiO_2 nanotubes with diameters of 30, 70 and 100 nm in promoting peri-implant bone formation by using pig as animal model are being studied by Wang et al. [98]. In their work, the nanotubes were crystallized into anatase structure after heat treatment at 500 °C for 2 h. Gene expression of Osterix (OSX), ALP, collagen type-1 (Col-I) and tartrate-resistant acid phosphate (TRAP) and histological analysis were evaluated. OSX is a zinc finger transcription factor expressed by osteoblasts which is vital for osteoblast differentiation. TRAP is reported to be expressed in osteoclasts at high level and thereby is used as bone resorption marker [99]. Based on the results, the expression of OSX, Col-I, ALP and TRAP was significantly higher on the TiO_2 nanotube implant surfaces when compared to the control Ti implant surface. Among the tube diameters, 70 nm TiO_2 nanotubes exhibited the highest level of gene expression, suggesting that 70 nm was an optimum size for osteoblast differentiation, matrix formation and mineralization. The high expression of bone formation and bone resorption markers indicated an active formation and remodelling concomitant with an increasing osteointegration of TiO_2 nanotubes implant to bone. From the histomorphometry analysis, bone-implant contact (BIC) was found to increase on TiO_2 nanotube surface, especially on implants with 70 nm TiO_2 nanotubes. In summary, these findings suggest that 70 nm nanotube is the optimum size for implantation to obtain the desired osteoconductivity and osteointegration.

4. Future directions

The literature presented in this review clearly indicates the efficacy of TiO_2 nanotube structures in eliciting cellular response in terms of adhesion, proliferation and differentiation by varying its tube diameter, crystallinity and length. This nanotubular structure provides topographical cues and signals to guide cell functionality of different cell lineages. Much of the future work in the TiO_2 nanotube field is focused on filling the nanotube pores with bioactive molecules for enhanced biomedical application such as development of controlled drug delivery system. Future growth of research interest in TiO_2 nanostructures is anticipated in the area of TiO_2 nanofibers. A few studies reported that TiO_2 nanofibers present a topography that has morphological similarity to natural extracellular matrix and they are thermodynamically more stable than TiO_2 nanotube structure [100–106]. Dong et al. [42] has fabricated TiO_2 nanofiber scaffold by using hydrothermal reaction and the results showed that mesenchymal stem cells were adhered well

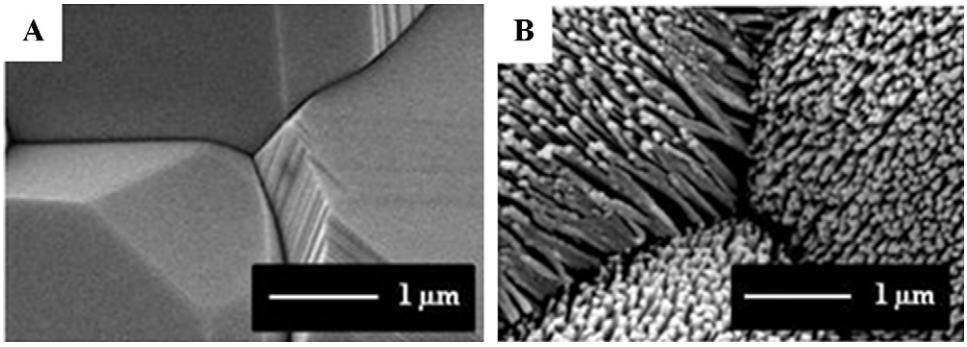

Fig. 6. SEM micrographs of a TiO_2 polycrystalline sample as-prepared (A) and after treatment in 5% H_2–95% N_2 gas environment at 700 °C for 8 h (B). Oriented nanofibers of TiO_2 are formed by a 'nano-carving' process involving etching by H_2 gas [108].
Reprinted with permission from John Wiley and Sons Inc.

on the nanofiber scaffold. Wang et al. reported that the titanium surface with nanofiber morphology showed better apatite-inducing ability compared to those surfaces with nanoporous and nanoplate morphology by conducting *in vitro* simulated body fluid test [107]. In a recent study by Tavangar et al. [102], 3-D TiO_2 nanofibrous structure was synthesized on Ti substrate by using femtosecond laser irradiation. Uniform apatite precipitation was observed on the nanofibrous structure. EDX results showed the molar Ca/P ratio for the apatite layer was around 1.63, which corresponds to hydroxyapatite. It is therefore foreseen that TiO_2 nanofibrillar structures are potential candidates for the future development in various biomedical applications. To that end, there has been some recent development in the fabrication of oriented TiO_2 nanofibers by very inexpensive and highly scalable surface modification techniques involving gas-phase reactions [108–111]. Some representative nanofiber structures are shown in Figs. 6 and 7. It would be interesting to explore cellular response on these platforms since their fabrication is simple and inexpensive.

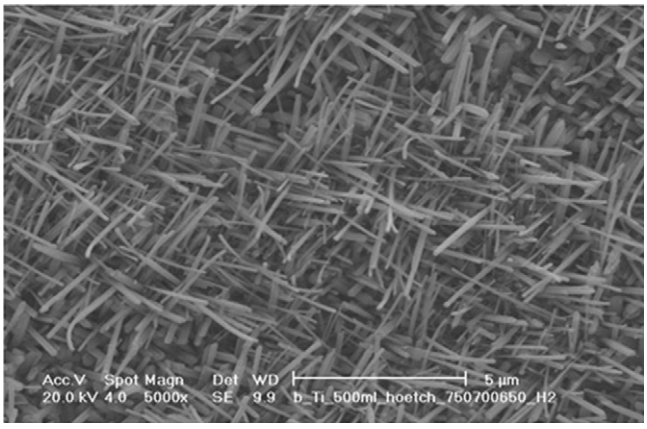

Fig. 7. SEM micrograph of TiO_2 nanofibers grown on β-Ti (5-5-5) alloy in Ar atmosphere (containing 10 s of ppm of O_2) at 700 °C for 8 h *via* a thermal oxidation process. The growth of nanowires on (110) grain shows that the directions of nanowires are perpendicular to each other [111].
Reprinted with permission from Ref. [111]. Copyright 2011, American Institute of Physics.

References

[1] W.Q. Yu, Y.L. Zhang, X.Q. Jiang, F.Q. Zhang, In vitro behavior of MC3T3-E1 preosteoblast with different annealing temperature titania nanotubes, Oral Dis. 16 (7) (2010) 624–630.
[2] K. Das, S. Bose, A. Bandyopadhyay, TiO2 nanotubes on Ti: influence of nanoscale morphology on bone cell-materials interaction, J. Biomed. Mater. Res. A 90 (1) (2009) 225–237.
[3] Z.X. Chen, Y. Takao, W.X. Wang, T. Matsubara, L.M. Ren, Surface characteristics and in vitro biocompatibility of titanium anodized in a phosphoric acid solution at different voltages, Biomed. Mater. 4 (6) (2009).
[4] W.Q. Yu, J. Qui, L. Xu, F.Q. Zhang, Corrosion behaviors of TiO(2) nanotube layers on titanium in Hank's solution, Biomed. Mater. 4 (6) (2009).
[5] G.J. Chen, Z. Wang, H. Bai, J.M. Li, H. Cai, A preliminary study on investigating the attachment of soft tissue onto micro-arc oxidized titanium alloy implants, Biomed. Mater. 4 (1) (2009).
[6] H. Kim, S.H. Choi, J.J.. Ryu, S.Y. Koh, J.H. Park, I.S. Lee, The biocompatibility of SLA-treated titanium implants, Biomed. Mater. 3 (2) (2008).
[7] X. Hu, H. Shen, K. Shuai, E. Zhang, Y. Bai, Y. Cheng, X. Xiong, S. Wang, J. Fang, S. Wei, Surface bioactivity modification of titanium by CO2 plasma treatment and induction of hydroxyapatite: in vitro and in vivo studies, Appl. Surf. Sci. 257 (6) (2011) 1813–1823.
[8] M.P. Bajgai, D.C. Parajuli, S.J. Park, K.H. Chu, H.S. Kang, H.Y. Kim, In vitro bioactivity of sol-gel-derived hydroxyapatite particulate nanofiber modified titanium, J. Mater. Sci. Mater. Med. 21 (2) (2010) 685–694.
[9] M.H. Hong, D.H. Lee, K.M. Kim, Y.K. Lee, Improved bonding strength between TiO2 film and Ti substrate by microarc oxidation, Surf. Interf. Analysis 42 (6–7) (2010) 492–496.
[10] Y. Bai, I.S. Park, H.H. Park, M.H. Lee, T.S. Bae, W. Duncan, M. Swain, The effect of annealing temperatures on surface properties, hydroxyapatite growth and cell behaviors of TiO2 nanotubes, Surf. Interf. Analysis 43 (6) (2011) 998–1005.
[11] W.Q. Yu, X.Q. Jiang, F.Q. Zhang, L. Xu, The effect of anatase TiO2 nanotube layers on MC3T3-E1 preosteoblast adhesion, proliferation, and differentiation, J. Biomed. Mater. Res. A 94 (4) (2010) 1012–1022.
[12] J. Lim, B. Yu, K. Woo, Y. Lee, Immobilization of TiO2 nanofibers on titanium plates for implant applications, Appl. Surf. Sci. 255 (5) (2008) 2456–2460.
[13] C.Y. Wang, B.H. Zhao, H.J. Ai, Y.W. Wang, Comparison of biological characteristics of mesenchymal stem cells grown on two different titanium implant surfaces, Biomed. Mater. 3 (1) (2008).
[14] E.W. Zhang, Y.B. Wang, K.G. Shuai, F. Gao, Y.J. Bai, Y. Cheng, X.L. Xiong, Y.F. Zheng, S.C. Wei, In vitro and in vivo evaluation of SLA titanium surfaces with further alkali or hydrogen peroxide and heat treatment, Biomed. Mater. 6 (2) (2011).

[15] A. Wennerberg, T. Albrektsson, C. Johansson, B. Andersson, Experimental study of turned and grit-blasted screw-shaped implants with special emphasis on effects of blasting material and surface topography, Biomaterials 17 (1) (1996) 15–22.
[16] S. Nishiguchi, H. Kato, H. Fujita, M. Oka, H.M. Kim, T. Kokubo, T. Nakamura, Titanium metals form direct bonding to bone after alkali and heat treatments, Biomaterials 22 (18) (2001) 2525–2533.
[17] S. Ban, Y. Iwaya, H. Kono, H. Sato, Surface modification of titanium by etching in concentrated sulfuric acid, Dental Mater. 22 (12) (2006) 1115–1120.
[18] H.-W. Kim, Y.-H. Koh, L.-H. Li, S. Lee, H.-E. Kim, Hydroxyapatite coating on titanium substrate with titania buffer layer processed by sol-gel method, Biomaterials 25 (13) (2004) 2533–2538.
[19] B. Yang, M. Uchida, H.-M. Kim, X. Zhang, T. Kokubo, Preparation of bioactive titanium metal via anodic oxidation treatment, Biomaterials 25 (6) (2004) 1003–1010.
[20] D. Krupa, J. Baszkiewicz, J. Zdunek, J. Smolik, Z. Slomka, J.W. Sobczak, Characterization of the surface layers formed on titanium by plasma electrolytic oxidation, Surf. Coat. Technol. 205 (6) (2010) 1743–1749.
[21] H.-J. Song, S.-H.. Park, S.-H. Jeong, Y.-J. Park, Surface characteristics and bioactivity of oxide films formed by anodic spark oxidation on titanium in different electrolytes, J. Mater. Process. Technol. 209 (2) (2009) 864–870.
[22] S.W.K. Kweh, K.A. Khor, P. Cheang, An in vitro investigation of plasma sprayed hydroxyapatite (HA) coatings produced with flame-spheroidized feedstock, Biomaterials 23 (3) (2002) 775–785.
[23] H. Baumann, K. Bethge, G. Bilger, D. Jones, I. Symietz, Thin hydroxyapatite surface layers on titanium produced by ion implantation, Nuclear Instrum. Methods Phys. Res. Sect. B: Beam Interact. Mater. Atoms 196 (3–4) (2002) 286–292.
[24] L.M. Bjursten, L. Rasmusson, S. Oh, G.C. Smith, K.S. Brammer, S. Jin, Titanium dioxide nanotubes enhance bone bondingin vivo, J. Biomed. Mater. Res. Part A 9999A (2009).
[25] S. Oh, C. Daraio, L.H. Chen, T.R. Pisanic, R.R. Finones, S. Jin, Significantly accelerated osteoblast cell growth on aligned TiO2 nanotubes, J. Biomed. Mater. Res. A 78 (1) (2006) 97–103.
[26] W.Q. Yu, J. Qiu, F.Q. Zhang, In vitro corrosion study of different TiO2 nanotube layers on titanium in solution with serum proteins, Colloids Surf. B Biointerfaces 84 (2) (2011) 400–405.
[27] N. Swami, Z. Cui, L.S. Nair, Titania Nanotubes, Novel nanostructures for improved osseointegration, J. Heat Transfer 133 (3) (2011) 034002.
[28] H.M. Kim, W.P. Chae, K.W. Chang, S. Chun, S. Kim, Y. Jeong, I.K. Kang, Composite nanofiber mats consisting of hydroxyapatite and titania for biomedical applications, J. Biomed. Mater. Res. B Appl. Biomater. 94 (2) (2010) 380–387.
[29] T.J. Webster, C. Ergun, R.H. Doremus, R.W. Siegel, R. Bizios, Enhanced functions of osteoblasts on nanophase ceramics, Biomaterials 21 (17) (2000) 1803–1810.
[30] T.J. Webster, J.U. Ejiofor, Increased osteoblast adhesion on nanophase metals: Ti, Ti6Al4V, and CoCrMo, Biomaterials 25 (19) (2004) 4731–4739.
[31] A. Simchi, E. Tamjid, F. Pishbin, A.R. Boccaccini, Recent progress in inorganic and composite coatings with bactericidal capability for orthopaedic applications, Nanomedicine 7 (1) (2011) 22–39.
[32] S. Oh, K.S. Brammer, Y.S. Li, D. Teng, A.J. Engler, S. Chien, S. Jin, Stem cell fate dictated solely by altered nanotube dimension, Proc. Natl. Acad. Sci. U.S.A. 106 (7) (2009) 2130–2135.
[33] K.S. Brammer, S. Oh, C.J. Cobb, L.M. Bjursten, H. van der Heyde, S. Jin, Improved bone-forming functionality on diameter-controlled TiO(2) nanotube surface, Acta Biomater. 5 (8) (2009) 3215–3223.
[34] S. Liu, A. Chen, Coadsorption of horseradish peroxidase with thionine on TiO_2 nanotubes for biosensing, Langmuir 21 (18) (2005) 8409–8413.
[35] K. Shankar, G.K. Mor, H.E. Prakasam, O.K. Varghese, C.A. Grimes, Self-assembled hybrid polymer - TiO2 nanotube array heterojunction solar cells, Langmuir 23 (24) (2007) 12445–12449.
[36] S.P. Albu, A. Ghicov, J.M. Macak, R. Hahn, P. Schmuki, Self-organized free-standing TiO2 nanotube membrane for flow-through photocatalytic applications, Nano Letters 7 (5) (2007) 1286–1289.
[37] A. Hu, X. Zhang, K.D. Oakes, P. Peng, Y.N. Zhou, M.R. Servos, Hydrothermal growth of free standing TiO2 nanowire membranes for photocatalytic degradation of pharmaceuticals, J. Hazard. Mater. 189 (1-2) (2011) 278–285.
[38] M. Paulose, K. Shankar, S. Yoriya, H.E. Prakasam, O.K. Varghese, G.K. Mor, T.A. Latempa, A. Fitzgerald, C.A. Grimes, Anodic growth of highly ordered TiO2 nanotube arrays to 134 m in length, J. Phys. Chem. B 110 (33) (2006) 16179–16184.
[39] M. Bigerelle, K. Anselme, B. Noël, I. Ruderman, P. Hardouin, A. Iost, Improvement in the morphology of Ti-based surfaces: a new process to increase in vitro human osteoblast response, Biomaterials 23 (7) (2002) 1563–1577.
[40] K.S. Brammer, S. Oh, J.O. Gallagher, S. Jin, Enhanced cellular mobility guided by TiO2 nanotube surfaces, Nano Letters 8 (3) (2008) 786–793.
[41] K.S. Brammer, C. Choi, C.J. Frandsen, S. Oh, G. Johnston, S. Jin, Comparative cell behavior on carbon-coated TiO2 nanotube surfaces for osteoblasts vs. osteo-progenitor cells, Acta Biomater. 7 (6) (2011) 2697–2703.
[42] W. Dong, T. Zhang, M. McDonald, C. Padilla, J. Epstein, Z.R. Tian, Biocompatible nanofiber scaffolds on metal for controlled release and cell colonization, Nanomedicine 2 (4) (2006) 248–252.
[43] Z. Huang, R.H. Daniels, R.J. Enzerink, V. Hardev, V. Sahi, S.B. Goodman, Effect of nanofiber-coated surfaces on the proliferation and differentiation of osteoprogenitors in vitro, Tissue Eng. Part A 14 (11) (2008) 1853–1859.
[44] W. Dong, T. Zhang, J. Epstein, L. Cooney, H. Wang, Y. Li, Y.B. Jiang, A. Cogbill, V. Varadan, Z.R. Tian, Multifunctional nanowire bioscaffolds on titanium, Chem. Mat. 19 (18) (2007) 4454–4459.
[45] P. Hoyer, Formation of a titanium dioxide nanotube array, Langmuir 12 (6) (1996) 1411–1413.
[46] J.H. Jung, H. Kobayashi, K.J.C. van Bommel, S. Shinkai, T. Shimizu, Creation of novel helical ribbon and double-layered nanotube TiO2 structures using an organogel template, Chem. Mat. 14 (4) (2002) 1445–1447.
[47] J.-H. Lee, I.-C. Leu, M.-C. Hsu, Y.-W. Chung, M.-H. Hon, Fabrication of aligned TiO2 one-dimensional nanostructured arrays using a one-step templating solution approach, J. Phys. Chem. B 109 (27) (2005) 13056–13059.
[48] D. Gong, C.A. Grimes, O.K. Varghese, W. Hu, R.S. Singh, Z. Chen, E.C. Dickey, Titanium oxide nanotube arrays prepared by anodic oxidation, J. Mater. Res. 16 (12) (2001) 3331–3334.
[49] A. Ghicov, H. Tsuchiya, J.M. Macak, P. Schmuki, Titanium oxide nanotubes prepared in phosphate electrolytes, Electrochem. Commun. 7 (5) (2005) 505–509.
[50] O.K. Varghese, D. Gong, M. Paulose, C.A. Grimes, E.C. Dickey, Crystallization and high-temperature structural stability of titanium oxide nanotube arrays, J. Mater. Res. 18 (01) (2003) 156–165.
[51] C.-C. Tsai, H. Teng, Regulation of the physical characteristics of titania nanotube aggregates synthesized from hydrothermal treatment, Chem. Mat. 16 (22) (2004) 4352–4358.
[52] C.-C. Tsai, H. Teng, Structural features of nanotubes synthesized from NaOH treatment on TiO2 with different post-treatments, Chem. Mat. 18 (2) (2005) 367–373.
[53] C.-C. Tsai, J.-N. Nian, H. Teng, Mesoporous nanotube aggregates obtained from hydrothermally treating TiO2 with NaOH, Appl. Surf. Sci. 253 (4) (2006) 1898–1902.
[54] B. Poudel, W.Z. Wang, C. Dames, J.Y. Huang, S. Kunwar, D.Z. Wang, D. Banerjee, G. Chen, Z.F. Ren, Formation of crystallized titania nanotubes and their transformation into nanowires, Nanotechnology 16 (9) (2005) 1935–1940.
[55] J. Yu, H. Yu, B. Cheng, X. Zhao, Q. Zhang, Preparation and photocatalytic activity of mesoporous anatase TiO2 nanofibers by a hydrothermal method, J. Photochem. Photobiol. A: Chem. 182 (2) (2006) 121–127.
[56] C. Bae, H. Yoo, S. Kim, K. Lee, J. Kim, M.M. Sung, H. Shin, Template-directed synthesis of oxide nanotubes: fabrication, characterization, and applications, Chem. Mat. 20 (3) (2008) 756–767.
[57] H.-H. Ou, S.-L. Lo, Review of titania nanotubes synthesized via the hydrothermal treatment: fabrication, modification, and application, Sep. Purif. Technol. 58 (1) (2007) 179–191.

[58] J.J. Qiu, W.D. Yu, X.D. Gao, X.M. Li, Sol-gel assisted ZnO nanorod array template to synthesize TiO2 nanotube arrays, Nanotechnology 17 (18) (2006) 4695–4698.
[59] M. Zhang, Y. Bando, K. Wada, Sol-gel template preparation of TiO2 nanotubes and nanorods, J. Mater. Sci. Lett. 20 (2) (2001) 167–170.
[60] X.H. Li, W.M. Liu, H.L. Li, Template synthesis of well-aligned titanium dioxide nanotubes, Appl. Phys. A-Mater. Sci. Process. 80 (2) (2005) 317–320.
[61] T. Maiyalagan, B. Viswanathan, U.V. Varadaraju, Fabrication and characterization of uniform TiO2 nanotube arrays by sol-gel template method, Bull. Mat. Sci. 29 (7) (2006) 705–708.
[62] T. Kasuga, M. Hiramatsu, A. Hoson, T. Sekino, K. Niihara, Formation of titanium oxide nanotube, Langmuir 14 (12) (1998) 3160–3163.
[63] C.L. Wong, Y.N. Tan, A.R. Mohamed, A review on the formation of titania nanotube photocatalysts by hydrothermal treatment, J. Environ. Manage. 92 (7) (2011) 1669–1680.
[64] J. Park, Y. Ryu, H. Kim, C. Yu, Simple, fast annealing synthesis of titanium dioxide nanostructures and morphology transformation during annealing processes, Nanotechnology 20 (10) (2009) 105608.
[65] S. Bauer, S. Kleber, P. Schmuki, TiO2 nanotubes: tailoring the geometry in H3PO4/HF electrolytes, Electrochem. Commun. 8 (8) (2006) 1321–1325.
[66] Z.V. Saponjic, N.M. Dimitrijevic, D.M. Tiede, A.J. Goshe, X. Zuo, L.X. Chen, A.S. Barnard, P. Zapol, L. Curtiss, T. Rajh, Shaping nanometer-scale architecture through surface chemistry, Adv. Mater. 17 (8) (2005) 965–971.
[67] Y. Ma, Y. Lin, X. Xiao, X. Zhou, X. Li, Sonication-hydrothermal combination technique for the synthesis of titanate nanotubes from commercially available precursors, Mater. Res. Bull. 41 (2) (2006) 237–243.
[68] N. Viriya-empikul, T. Charinpanitkul, N. Sano, A. Soottitantawat, T. Kikuchi, K. Faungnawakij, W. Tanthapanichakoon, Effect of preparation variables on morphology and anatase-brookite phase transition in sonication assisted hydrothermal reaction for synthesis of titanate nanostructures, Mater. Chem. Phys. 118 (1) (2009) 254–258.
[69] Z.-Y. Yuan, B.-L.. Su, Titanium oxide nanotubes, nanofibers and nanowires, Colloids Surf. A: Physicochem. Eng. Aspects 541 (1–3) (2004) 173–183.
[70] A.-L. Papa, N. Millot, L. Saviot, R. m. Chassagnon, O. Heintz, Effect of reaction parameters on composition and morphology of titanate nanomaterials, J. Phys. Chem. C 113 (29) (2009) 12682–12689.
[71] S. Sreekantan, L.C. Wei, Study on the formation and photocatalytic activity of titanate nanotubes synthesized via hydrothermal method, J. Alloys Compd. 490 (1-2) (2010) 436–442.
[72] Y. Lan, X.P. Gao, H.Y. Zhu, Z.F. Zheng, T.Y. Yan, F. Wu, S.P. Ringer, D.Y. Song, Titanate nanotubes nanorods prepared from rutile powder, Adv. Funct. Mater. 15 (8) (2005) 1310–1318.
[73] Z.-Y. Yuan, W. Zhou, B.-L. Su, Hierarchical interlinked structure of titanium oxide nanofibers, Chem. Commun. 11 (2002) 1202–1203.
[74] T. Kasuga, M. Hiramatsu, A. Hoson, T. Sekino, K. Niihara, Titania nanotubes prepared by chemical processing, Adv. Mater. 11 (15) (1999) 1307–1311.
[75] X. Sun, Y. Li, Synthesis and characterization of ion-exchangeable titanate nanotubes, Chem.–Eur. J. 9 (10) (2003) 2229–2238.
[76] J. Yang, Z. Jin, X. Wang, W. Li, J. Zhang, S. Zhang, X. Guo, Z. Zhang, Study on composition, structure and formation process of nanotube Na2Ti2O4(OH)2, Dalton Trans. (20) (2003) 3898–3901.
[77] Q. Chen, G.H. Du, S. Zhang, L.-M. Peng, The structure of trititanate nanotubes, Acta Crystall. Sect. B 58 (4) (2002) 587–593.
[78] G.H. Du, Q. Chen, R.C. Che, Z.Y. Yuan, L.M. Peng, Preparation, structure analysis of titanium oxide nanotubes, Appl. Phys. Lett. 79 (22) (2001) 3702–3704.
[79] Z. Lin, I.S. Lee, Y.J. Choi, I.S. Noh, S.M. Chung, Characterizations of the TiO(2-x) films synthesized by e-beam evaporation for endovascular applications, Biomed. Mater. 4 (1) (2009).
[80] M.M. Barreiro, D.R. Grana, G.A. Kokubu, M.I. Luppo, S. Mintzer, G. Vigna, Titanium compacts produced by the pulvimetallurgical hydride-dehydride method for biomedical applications, Biomed. Mater. 5 (2) (2010).
[81] S. Oh, S. Jin, Titanium oxide nanotubes with controlled morphology for enhanced bone growth, Mater. Sci. Eng. C 26 (8) (2006) 1301–1306.
[82] J. Park, S. Bauer, K.A. Schlegel, F.W. Neukam, K. von der Mark, P. Schmuki, TiO_2 nanotube surfaces: 15 nm—an optimal length scale of surface topography for cell adhesion and differentiation, Small 5 (6) (2009) 666–671.
[83] T. Sjöström, G. Lalev, J.P. Mansell, B. Su, Initial attachment and spreading of MG63 cells on nanopatterned titanium surfaces via through-mask anodization, Appl. Surf. Sci. 257 (10) (2011) 4552–4558.
[84] B.S. Smith, S. Yoriya, T. Johnson, K.C. Popat, Dermal fibroblast and epidermal keratinocyte functionality on titania nanotube arrays, Acta Biomater. 7 (6) (2011) 2686–2696.
[85] K. Burns, C. Yao, T.J. Webster, Increased chondrocyte adhesion on nanotubular anodized titanium, J. Biomed. Mater. Res. Part A 88A (3) (2009) 561–568.
[86] K.S. Brammer, S. Oh, C.J Frandsen, S. Varghese, S. Jin, Nanotube surface triggers increased chondrocyte extracellular matrix production, Mater. Sci. Eng.: C 30 (4) (2010) 518–525.
[87] L. Peng, M.L. Eltgroth, T.J. LaTempa, C.A. Grimes, T.A. Desai, The effect of TiO_2 nanotubes on endothelial function and smooth muscle proliferation, Biomaterials 30 (7) (2009) 1268–1272.
[88] J. Park, S. Bauer, K. von der Mark, P. Schmuki, Nanosize and vitality: TiO_2 nanotube diameter directs cell fate, Nano Lett. 7 (6) (2007) 1686–1691.
[89] K.C. Popat, L. Leoni, C.A. Grimes, T.A. Desai, Influence of engineered titania nanotubular surfaces on bone cells, Biomaterials 28 (21) (2007) 3188–3197.
[90] S. Bauer, J. Park, K. von der Mark, P. Schmuki, Improved attachment of mesenchymal stem cells on super-hydrophobic TiO2 nanotubes, Acta Biomater. 4 (5) (2008) 1576–1582.
[91] S. Bauer, J. Park, J. Faltenbacher, S. Berger, K. von der Mark, P. Schmuki, Size selective behavior of mesenchymal stem cells on ZrO(2) and TiO(2) nanotube arrays, Integr. Biol. (Camb.) 1 (8–9) (2009) 525–532.
[92] M. Niinomi, Mechanical biocompatibilities of titanium alloys for biomedical applications, J. Mech. Behav. Biomed. Mater. 1 (1) (2008) 30–42.
[93] K. Wang, The use of titanium for medical applications in the USA, Mater. Sci. Eng. A 213 (1–2) (1996) 134–137.
[94] A.L. Rosa, M.M. Beloti, Rat bone marrow cell response to titanium and titanium alloy with different surface roughness, Clin. Oral Implant. Res. 14 (1) (2003) 43–49.
[95] J. Takagi, B.M. Petre, T. Walz, T.A. Springer, Global conformational rearrangements in integrin extracellular domains in outside-in and inside-out signaling, Cell 110 (5) (2002) 599–611.
[96] Y. Bai, S. Park, H.H. Park, M.H. Lee, T.S. Bae, W. Duncan, A. Swain, The effect of annealing temperatures on surface properties, hydroxyapatite growth and cell behaviors of TiO(2) nanotubes, Surf. Interface Analysis 43 (6) (2011) 998–1005.
[97] C. von Wilmowsky, S. Bauer, R. Lutz, M. Meisel, F.W. Neukam, T. Toyoshima, P. Schmuki, E. Nkenke, K.A. Schlegel, In vivo evaluation of anodic TiO2 nanotubes: an experimental study in the pig, J. Biomed. Mater. Res. Part B: Appl. Biomater. 89B (1) (2009) 165–171.
[98] N. Wang, H. Li, W. Lü, J. Li, J. Wang, Z. Zhang, Y. Liu, Effects of TiO_2 nanotubes with different diameters on gene expression and osseointegration of implants in minipigs, Biomaterials 32 (29) (2011) 6900–6911.
[99] C. Minkin, Bone acid phosphatase: tartrate-resistant acid phosphatase as a marker of osteoclast function, Calcified Tissue Int. 34 (3) (1982) 285–290.
[100] W.J. Li, C.T. Laurencin, E.J. Caterson, R.S. Tuan, F.K. Ko, Electrospun nanofibrous structure: a novel scaffold for tissue engineering, J. Biomed. Mater. Res. 60 (4) (2002) 613–621.
[101] E.M. Christenson, K.S. Anseth, L. van den Beucken, C.K. Chan, B. Ercan, J.A. Jansen, C.T. Laurencin, W.J. Li, R. Murugan, L.S. Nair, S. Ramakrishna, R.S. Tuan, T.J. Webster, A.G. Mikos, Nanobiomaterial applications in orthopedics, J. Orthop. Res. 25 (1) (2007) 11–22.
[102] A. Tavangar, B. Tan, K. Venkatakrishnan, Synthesis of bio-functionalized three-dimensional titania nanofibrous structures using femtosecond laser ablation, Acta Biomater. 7 (6) (2011) 2726–2732.

[103] D.V. Bavykin, F.C. Walsh, Elongated titanate nanostructures and their applications, Eur. J. Inorg. Chem. 8 (2009) 977–997.
[104] R. Yoshida, Y. Suzuki, S. Yoshikawa, Syntheses of TiO2(B) nanowires and TiO2 anatase nanowires by hydrothermal and post-heat treatments, J. Solid State Chem. 178 (7) (2005) 2179–2185.
[105] A.R. Chandrasekaran, J. Venugopal, S. Sundarrajan, S. Ramakrishna, Fabrication of a nanofibrous scaffold with improved bioactivity for culture of human dermal fibroblasts for skin regeneration, Biomed. Mater. 6 (1) (2011).
[106] S.G. Kumbar, R. James, S.P. Nukavarapu, C.T. Laurencin, Electrospun nanofiber scaffolds: engineering soft tissues, Biomed. Mater. 3 (3) (2008).
[107] X.J. Wang, Y.C. Li, J.G. Lin, Y. Yamada, P.D. Hodgson, C.E. Wen, In vitro bioactivity evaluation of titanium and niobium metals with different surface morphologies, Acta Biomater. 4 (5) (2008) 1530–1535.
[108] S. Yoo, S.A. Akbar, K.H. Sandhage, Nanocarving of bulk titania crystals into oriented arrays of single-crystal nanofibers via reaction with hydrogen-bearing gas, Adv. Mater. 16 (3) (2004) 260–264.
[109] S.V.N.T. Kuchibhatla, A.S. Karakoti, D. Bera, S. Seal, One dimensional nanostructured materials, Prog. Mater. Sci. 52 (5) (2007) 699–913.
[110] H. Lee, S. Dregia, S. Akbar, M. Alhoshan, Growth of 1-D TiO2 nanowires on Ti and Ti alloys by oxidation, J. Nanomater. 2010 (2010).
[111] S.A. Akbar, Nano-structured oxides: a materials approach, AIP Conf. Proc. 1370 (1) (2011) 54–60.